

High Performance Plasmas with the JET Pumped Divertor in JET

R W T König, S Ali-Arshad, M Bures, J P Christiansen,
H P L de Esch, G Fishpool, M von Hellermann, T Hender,
O N Jarvis, T T C Jones, K D Lawson¹, P J Lomas,
A C Maas, F B Marcus, M F F Nave, R Sartori, B Schunke,
P Smeulders, D Stork, A Taroni, P R Thomas, K Thomsen
and the JET Team.

JET Joint Undertaking, Abingdon, Oxfordshire, OX14 3EA, UK.

¹ UKAEA Fusion, Culham, Abingdon, Oxfordshire, OX14 3DB, UK.

"This document is intended for publication in the open literature. It is made available on the understanding that it may not be further circulated and extracts may not be published prior to publication of the original, without the consent of the Publications Officer, JET Joint Undertaking, Abingdon, Oxon, OX14 3EA, UK".

"Enquiries about Copyright and reproduction should be addressed to the Publications Officer, JET Joint Undertaking, Abingdon, Oxon, OX14 3EA".

High Performance Plasmas with the JET Pumped Divertor in JET

R W T König, S Ali-Arshad, M Bures, J P Christiansen, H P L de Esch, G Fishpool, M von Hellermann, T Hender, O N Jarvis, T T C Jones, K D Lawson¹, P J Lomas, A C Maas, F B Marcus, M F F Nave, R Sartori, B Schunke, P Smeulders, D Stork, A Taroni, P R Thomas, K Thomsen and the JET Team.

JET Joint Undertaking, Abingdon, Oxfordshire, OX14 3EA, UK.

¹ UKAEA Fusion, Culham, Abingdon, Oxfordshire, OX14 3DB, UK.

INTRODUCTION

During the shutdown, which ended early this year, internal divertor coils, a new toroidally continuous array of Carbon Fibre Composite (CFC) divertor tiles and a toroidally continuous cryo-pump have been installed, still allowing for operation at up to 6 MA. Since the next DT experiment in JET is planned at the end of 1996 it is necessary to optimise the fusion performance in the new JET pumped divertor configuration in regimes with steady state potential as well as in those with maximum fusion yield.

VESSEL CONDITIONING AND ITS IMPACT ON PLASMA PERFORMANCE

- Until October the JET-PD vessel was only baked and operated at 250 °C (now 320 °C) to avoid the possibility of damage to the divertor coil epoxy (old JET was baked to 350 °C and operated at 300 °C).
- The new divertor tiles are mounted on water cooled supports (kept at ~40 °C between pulses).
- Inner wall is now much less covered with carbon tiles and the outer wall is not at all covered with carbon tiles, except at the locations of the poloidal limiters, which replace the old belt limiters.

A cryo-pump has been installed with a measured speed of $170 \text{ m}^3\text{s}^{-1}$. In an experiment, in which the plasma density was held constant by gas-puffing (the result was found to be independent of fuelling position), a max. deuterium removal rate of $8 \cdot 10^{21} \text{ s}^{-1}$ in an Ohmic plasma with $\langle n_e \rangle = 4 \cdot 10^{19} \text{ m}^{-3}$ has been achieved [Cam94]. Moving the outer strike point of the plasma across the horizontal and up the vertical target plate by up to 20 cm away from optimum position, resulted in a reduction of the pumping efficiency by a factor of 2. Even 20 cm from the pump entrance the particle removal rate should therefore be high enough to cope with the maximum particle input from the NBI (at $P_{\text{NBI}} = 18 \text{ MW}$ about $1.5 \cdot 10^{21} \text{ s}^{-1}$). Pressure measurements during hot-ion ELM-free H-modes suggest pumping of the order of 60 % of the beam fuelling, whilst the average plasma bulk density is rising 1-1.2 times

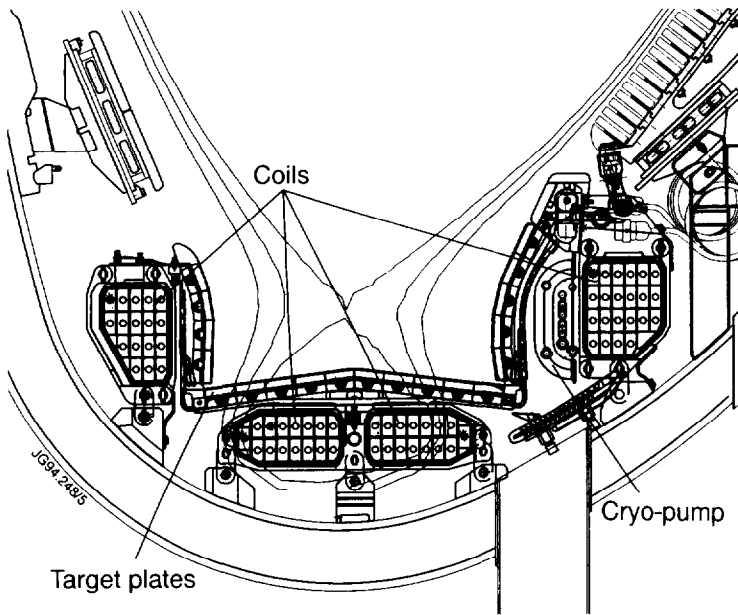


Fig. 1: Cross section of the JET Pumped Divertor showing the major components

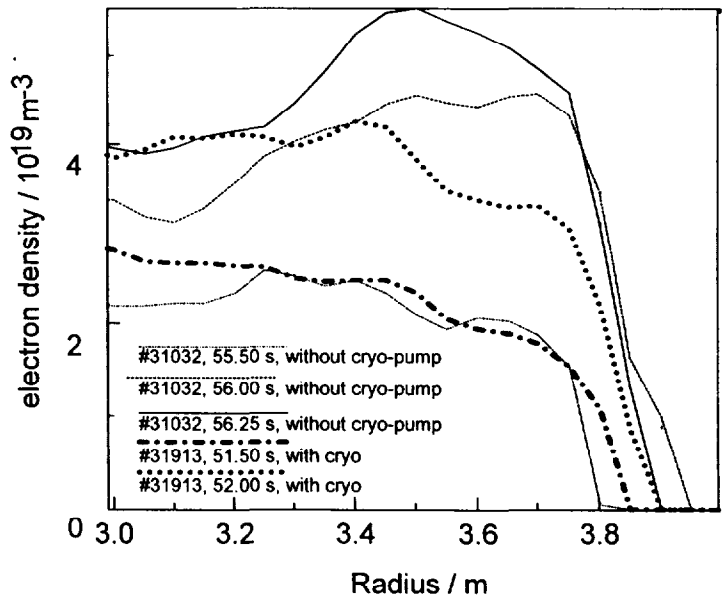


Fig. 2: Evolution of the electron density profiles with full cryo-pump (#31913, $P_{NBI} = 15$ MW) and without cryo-pump (#31032, $P_{NBI} = 13.5$ MW) for hot-ion mode plasmas from the beginning of the high power NBI heating phase onward until just before the end of the ELM-free period.

the beam fuelling. During the subsequent ELM phase the pumping can be as large as 9 times the beam fuelling (no gas fuelling), while the core plasma density is constant. Clearly a particle reservoir is being depleted.

- The vacuum conditions are very similar to those in previous campaigns and are even considerably better than previously when the divertor cryopump is used.
- To reduce the main chamber recycling in JET Be-evaporation (2 or 4 heads) plus He GDC is used. The fast density rise and the hollow density profiles during the ELM-free phase give a clear indication that the recycling in the new machine is considerably higher than in the old JET. First the use of half the cryo-pump and later of the full cryo-pump reduced the recycling sufficiently for the neutral beam fuelling to dominate the wall source. This then finally led to the peaked density profiles which are ideal for hot-ion modes due to the increased central beam deposition (Fig. 2).
- A tile heating experiment showed that increasing the divertor surface temperature to 1000 °C has little effect on the recycling. The subsequent high power ELM phase was unchanged whether or not sweeping was used to keep the tile temperature down.
- In hot-ion pulses a significantly higher neutral pressure was found in the divertor than in the midplane and following an ELM the pressure rises rapidly in the divertor but much more slowly at the midplane. This suggests that the neutrals arise in the divertor.

TERMINATION OF THE HIGH PERFORMANCE PHASE

Variety of termination scenarios (similar to the types observed in the old machine); these include

- fast terminations where a sawtooth is coupled to an ELM
- slow terminations where the confinement seems to be lost at the outer part of the plasma first and the limitation of the temperatures moves inward to the centre. Fig. 3 shows such a case which is clearly ELM limited.
- slow termination (neither sawtooth nor ELM(s)); in long ELM-free periods rising density and increasing radiation similar to old JET behaviour and ELM-free period often limited by return to L-mode (Fig. 4).
- but **no carbon bloom** as a result of good divertor design (usually $Z_{\text{eff}} < 2 - 2.5$)

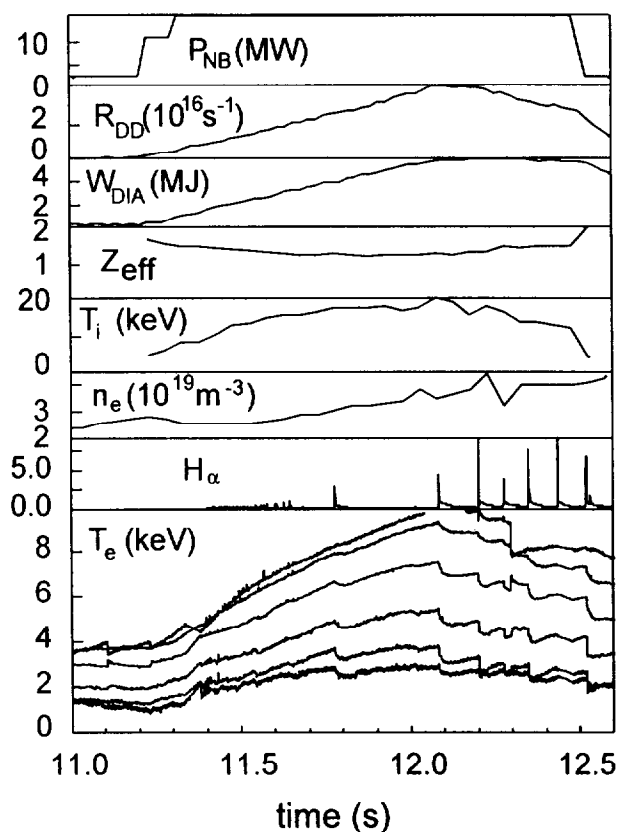


Fig. 3: Time traces for hot-ion pulse #31905 with low main chamber recycling obtained by cryo pumping for a standard fat plasma ($\delta=0.2$).

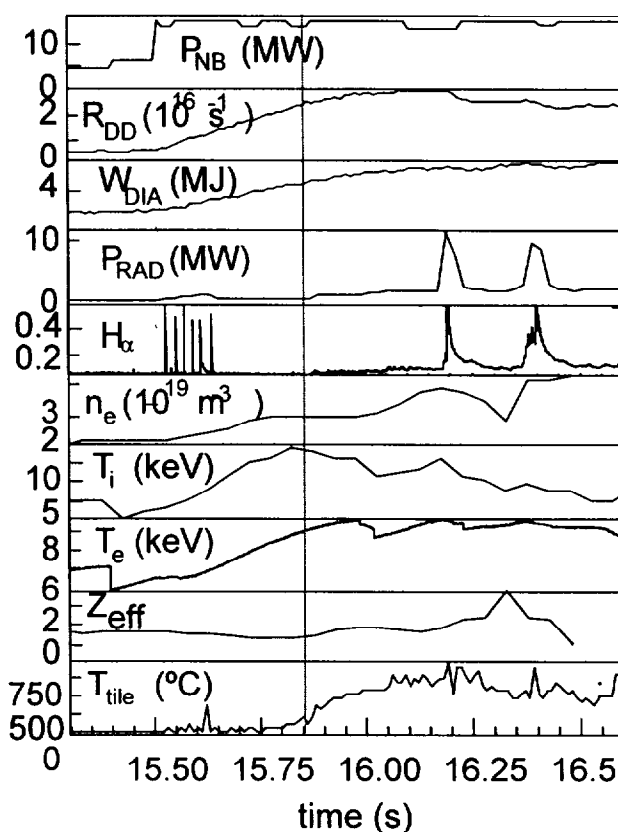


Fig. 4: Time traces for hot-ion pulse #31917 with low main chamber recycling obtained by cryo pumping for a high triangular plasma ($\delta=0.4$).

In the old JET

ELMs rarely found, they were only present just above the L-H transition threshold, with extremely strong gas puffing, at high beta or in hydrogen plasmas.

In the new JET-PD

ELMy H-modes are the norm in the high recycling conditions. Long ELM-free periods are difficult to achieve. ELMs have the characteristics of the 'giant' ELMs identified on DIII-D or ASDEX-U. The ELM frequency increases with input power and tends to reduce with plasma current. Experiments have shown that the ELM-free period is hardly influenced by different conditioning schemes, divertor tile heating, X-point to target distance, diverted plasma flux expansion, sweeping, or use of top X-point tiles [Lom94].

ELM-free period can be influenced by:

- minimum gas input to reduce recycling
- use of cryo-pump to reduce recycling
- triangularity (higher values increase edge shear which increases ideal ballooning limit to pressure gradient near the separatrix)
- A scan of elongation, triangularity and strike point location at constant power, plasma current, toroidal field and target density shows that increase of triangularity from 0.2 to 0.35 can extend ELM-free period from 0.3 to 2.0 sec. (high triangularity similar to old JET configurations)
- ELM-frequency increases strongly with power and decreases with plasma current in a similar manner to that observed on ASDEX and DIII-D.

present hypothesis: **"Proximity to ideal ballooning limit determines the ELM-free period."**

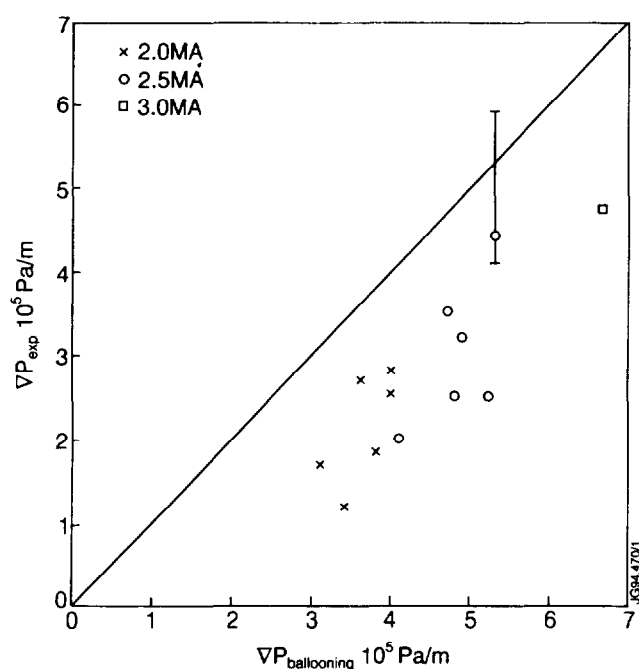


Fig. 5 Best estimate of the edge pressure limit against the calculated ideal ballooning limit. The upper limit of the error bar is the gradient one would get if the fall-off length were 3 cm

The theoretical pressure gradient limit has been calculated at 95% flux surface using EFIT reconstructions of plasma equilibria. Fig. 5 shows how close the gradients calculated from the outermost 3 LIDR points (5 cm resolution) are to the calculated Ballooning limit. The hypothesis is further supported by the fact that one also finds some of the right systematic dependencies like:

- ELM stability (i.e. the time between the L-H transition till the first ELM) seems to be improved by increased edge shear
- ELM stability is improved by increasing the triangularity of the equilibrium

If hypothesis is correct the ELM-free period is determined by the time to reach the edge ballooning limit.

CORRELATION BETWEEN GIANT ELMS AND FLUCTUATIONS

1. Magnetics

a) giant ELMs have long lived high frequency precursors (Fig. 6), which often saturate in amplitude before the ELMs. That means no direct cause and effect is observed between the precursor and the ELM.

b) giant ELMs also have low frequency precursors with a low n character

c) giant ELMs themselves have a strong low frequency low n component

During the ELM-free periods high frequency modes (>30 kHz) are observed. These modes, which have a complex frequency structure, appear with the L to H transition and disappear at the end of the H-mode.

The modes are modulated by giant ELMs and are saturated in high triangularity discharges (Fig. 7).

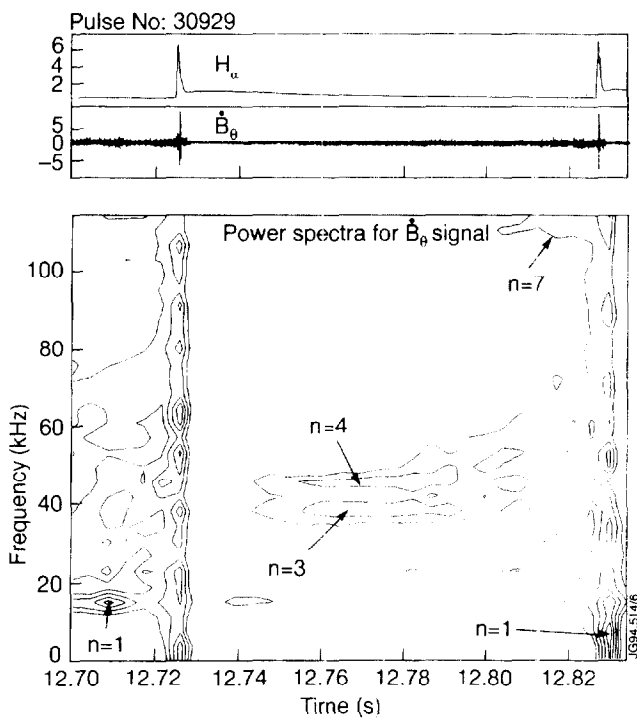


Fig. 6: High frequency precursor

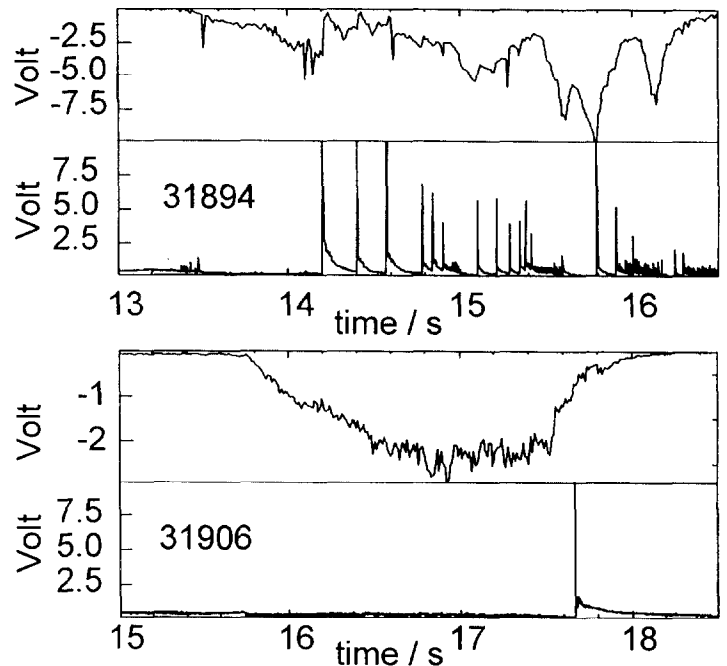


Fig. 7: Comparison of high frequency mode amplitudes (here at 43 kHz) for a low triangularity ($\delta=0.2$) plasma (#31894) and a high triangularity ($\delta=0.4$) plasma (#31906).

2. Reflectometer data analysis

a) high frequency precursor appears to move radially outwards

b) amplitude peaks near the plasma edge (chan 3 or $n_e = 1.06 \cdot 10^{19} \text{ m}^{-3}$)

c) high frequency precursor causes a flattening of the density profile near the edge [Col93]. The larger gradients at the edge of the plateau, created by the high frequency precursor, could then destabilise other modes.

d) the broad frequency band is short lived ($<1\text{ms}$) and finishes when H_α reaches the maximum; apart from the low frequencies the ELM is followed by a quiescent period over a certain radial range (Fig. 8). The broad band is mostly observed within the last 6 reflectometer channels ($<10\text{cm}$) although the ELM may be affecting T_e and T_i right through the plasma centre (Fig. 3).

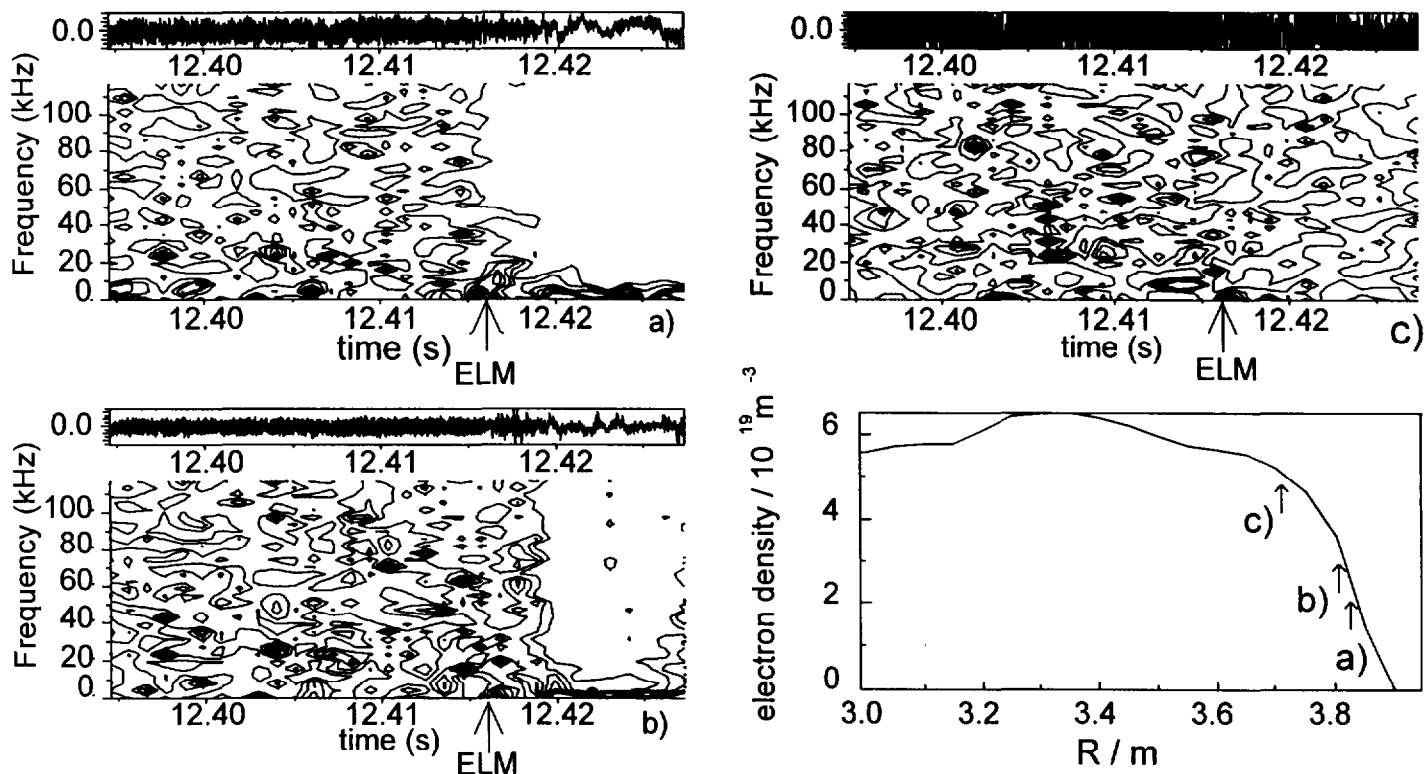


Fig. 8: A broad band of high frequency fluctuations is observed with the reflectometer just before the ELM (#31906). a) shows channel 6 which is representative for all other channels further outside (chan 1-5). At b) (chan 7) the quiescent period after the ELM starts to disappear while from chan 8 onward the quiescent period disappears totally. c) shown above corresponds to chan 9.

FUSION PERFORMANCE

Operating space

operated at $I_p = 1 - 4 \text{ MA}$ and $B_T = 1 - 3.4 \text{ T}$ in different configurations

L to H transition power threshold

essentially unchanged from the 1991/2 carbon tile campaign with grad \mathbf{B} drift towards the X-point (normal drift direction) and slightly lower than the old data with reversed grad \mathbf{B} direction

Performance

The $n\tau T$ -diagram in figure 9 shows the fusion performance that has been achieved so far with the new JET-PD in comparison with the old machine [Sto94]. The best 4MA/3.4T shot from this year is one of the best non hot ion modes achieved so far, obtained with 18 MW NBI heating. It would have $Q_{DT} \sim 0.1$ for a 0:50 D:T plasma mixture during the $\sim 2 \text{ s}$ ELMy phase. The best hot-ion H-mode discharge in the new machine has reached $n\tau T = 5.6 \cdot 10^{20} \text{ m}^{-3} \text{ s keV}$ which is about 60% of best previous value, $Q_{DT} \sim 0.6$.

Energy confinement in ELMy and ELM-free H-modes

The energy confinement time: over the range from 1 to 4 MA and toroidal fields from 1 to 3.4 T appears to be between 90 and 100 % of the ELM-free H-mode predictions (ITERH93-P). Fig. 10 shows a comparison of the measured diamagnetic energy confinement time versus the ITER89-P scaling for ELMy and ELM-free H-modes.

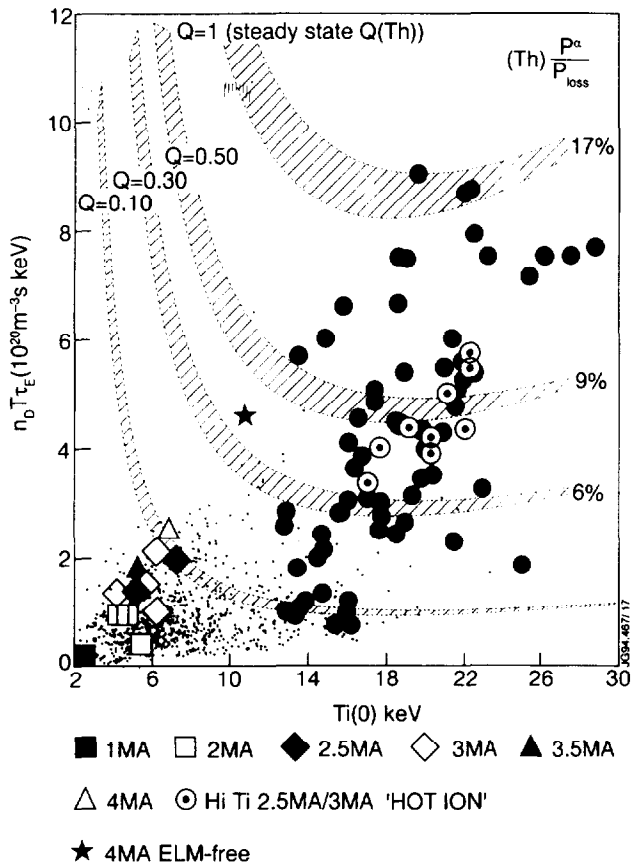


Fig. 9: Triple fusion product plotted against central ion temperature ($T_i(0)$) The JET-PD hot-ion H-modes are marked with open circles with a dot. The filled circles represent the 1991/92 hot-ion H-modes. The remaining data are JET-PD steady-state ($>4\tau_E$) H-modes.

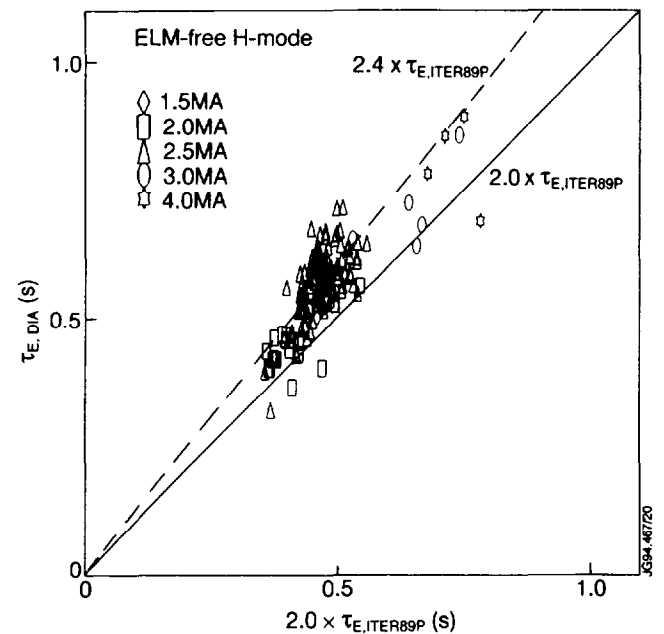
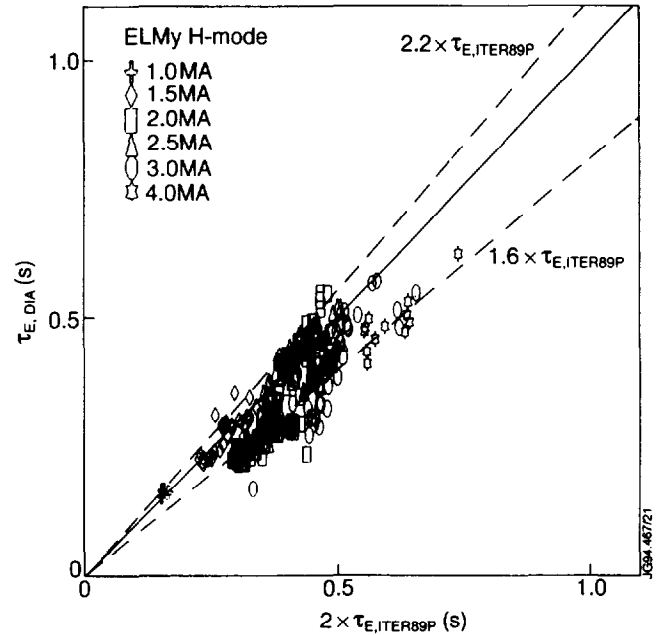


Fig. 10: Measured diamagnetic energy confinement time for the JET-PD ELMy and ELM-free H-mode dataset ($t_{\text{ELM-free}} > 0.5$ s) plotted against $2 \times$ the prediction from the ITER89-P scaling law. The ELM-free data selected have $dW/dt < 0.4 P_m$, the ELMy data $dW/dt < 0.1 P_m$.

Hot-ion H-modes

The hot-ion H-modes were optimised for high fusion yield for the PTE1 experiment in 1991. They were developed to a regime which showed VH-mode confinement (H-fact. >3 rel. to L-mode). It has been tried to regain that regime with the new JET-PD by optimising the 2.8T/2.5MA discharge (PTE: 2.8T/3.2MA).

a) Ion temperatures of $T_i(0) > 20$ keV have been reached with $T_i(0) > 2 T_e$ for up to 0.75 sec. The preparation of slightly peaked target density profiles by careful gas and pumping programming as well as the use of the cryo-pump is essential for the good beam penetration needed to achieve high central parameters and neutron yields. T_i and T_e values similar to those of the best 1991/2 shots were reached, but only about half the stored energy and neutron yield have been achieved. The highest DD reaction rate reached this year was $4.5 \cdot 10^{16} \text{ s}^{-1}$.

b) It seems that with the new JET-PD VH-mode confinement has not yet been achieved.

Possible reasons:

- still higher edge density gradients than in 1991/2 due to higher recycling
- edge plasma is not generating the levels of bootstrap current required for unconstrained access to the second stable region against ballooning modes, which has been identified as a signature of the VH-mode in JET and DIII-D. The hot-ion H-modes produced in with the new machine stand out from the rest of the ELM-free dataset as having enhanced confinement. The highest value reached so far in the new JET-PD is $2.9 \cdot \tau_{E, \text{ITER89-P}}$ (triang. $\delta=0.1-0.3$, old JET $\delta=0.35-0.5$).

CONCLUSIONS

Up to now H-mode divertor operation has been demonstrated at plasma currents up to 4 MA and in the hot-ion H-modes about half the performance of the best ones with the old machine have been achieved.

In contrast to the old machine in which it was difficult to produce ELMs, the H-modes in the new JET-PD are typically either ELMy with steady state density and confinement close to ELM-free values or have an early ELM-free period, the length of which can be influenced, during which the density rises very fast due to the, for reasons which are still not understood, considerably higher recycling in the new machine. Due to the good divertor design the performance of JET is no longer limited by the carbon bloom.

REFERENCES

[Cam94] D Campbell, IAEA Conference 1994, IAEA-CN-60/A-4-I-4

[Col93] A Colton, Ph. D thesis, Riso National Laboratory Report Riso-R-700(EN), 1993

[Lom94] P Lomas. IAEA Conference 1994, IAEA-CN-60/A-2-I-4

[Sto94] D Stork, IAEA Conference 1994, IAEA-CN-60/A-1-I-3